

## Chapter 18

# Applications of Quantum Dots for Fluorescence Imaging in Biomedical Research

*ShuQi Wang\**, *Matin Esfahani\**, *Dusan Sarenac\**,  
*Bettina Cheung\**, *Aishwarya Vasudevan\**, *Fatih Inci\**,  
and *Utkan Demirci\*<sup>†‡</sup>*

*\*Bio-Acoustic-MEMS in Medicine (BAMM) Laboratory  
Division of Biomedical Engineering, Department of Medicine  
Brigham and Women's Hospital, Harvard Medical School  
Boston, MA 02139, USA*

*†Harvard–MIT Health Sciences and Technology  
Cambridge, MA 02139, USA*

### Introduction

Biomedical research is currently one of the fastest growing areas with advanced technologies such as microfluidics, fluorescence imaging, and microelectromechanical systems (MEMS). For fluorescence imaging, conventional organic dyes (e.g., Rhodamine B) are extensively used.<sup>1,2</sup> Recently, quantum dots (QDs), due to their special optical properties,<sup>3</sup> are gaining momentum in their role in biomedical research such as in the development of biosensors, clinical diagnosis, and basic immunological studies.<sup>4–9</sup> QDs are semiconductor nanoparticles with a diameter of 5–50 nm, including a metal core and an insulator surface. Because of their nanoscale structure, QDs have strictly confined electronic wave functions,<sup>9,10</sup> which confer QDs with unique optical properties such as high luminescence intensity, high molar extinction coefficient, size-tunable emission

---

<sup>‡</sup>Corresponding author. Email: [udemirci@rics.bwh.harvard.edu](mailto:udemirci@rics.bwh.harvard.edu)

wavelengths, broad absorption spectra, and narrow emission bands. These properties enable applications such as the labeling of cells, antibodies, proteins, and viral particles for *in vitro* and *in vivo* studies. The ability to introduce QDs into cells allows the binding of QDs to subcellular components without affecting cellular integrity and thus, facilitates the study on protein–protein interactions (e.g., cell signaling pathways) at the subcellular level.<sup>11</sup> Along with the fast development of QD technologies, increasing concerns on the toxicity of QDs to human beings, animals, plants, as well the environment need to be addressed. In this chapter, the special optical properties of QDs, bioconjugation methods to facilitate fluorescence imaging, and applications of QDs in biomedical research are presented. In addition, the toxicity and biosafety of QDs for further clinical applications will be discussed.

### *Optical properties of QDs*

One of the most important features of QDs is the tunable wavelengths of emitted fluorescence.<sup>12</sup> QDs, as semiconductors, require an intermediate amount of energy to transport electrons in the conduction band. This energy is called the bandgap. Once the bandgap energy is overcome, electrons are excited. These electrons will revert to their initial state and emit photons in the form of fluorescence. The wavelength of emitted fluorescence largely depends on the bandgap size, which is governed by the size of QDs known as the quantum confinement effect.<sup>13,14</sup> The smaller the size of QDs, the shorter the wavelength of fluorescence they emit. Thus, it is possible to adjust the emission wavelengths of QDs by changing their size (Fig. 1).

Another important feature of QDs is their broad absorption and narrow emission wavelengths. The peaks of wavelength depend on the bandgap level. Since there are different values for bandgaps, the absorption spectra contain a number of overlapping peaks (Fig. 1). The energy absorbed by QDs typically decreases with increasing wavelengths of the excitation light source.<sup>15</sup> The maximum wavelength at which QDs absorb is called the absorption onset. The absorption spectrum of QDs can be observed at wavelengths from the ultraviolet (UV) region to the near-infrared (IR) region until the absorption onset.<sup>15</sup> This is particularly useful for multicolor biological labeling, where QDs with different emission wavelengths can be excited simultaneously.<sup>5,16</sup> The spectra of QDs can be sharp, narrow, and bell-shaped (Gaussian). This clear differentiation between the peaks of emitted fluorescence allows for multicolor staining, and the fluorescence peaks can be easily detected using different fluorescence filters. In contrast, organic dyes have overlapping fluorescence signals and the peaks are hardly distinguishable.

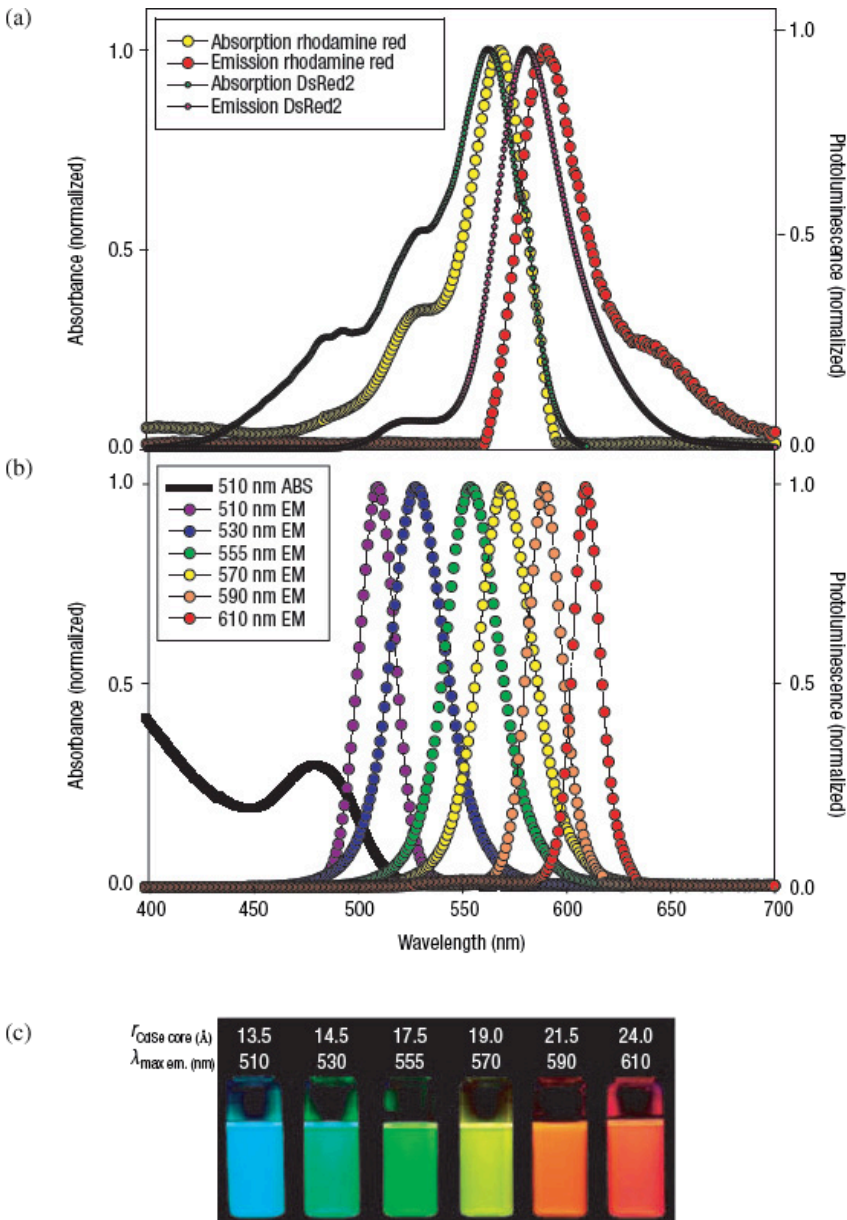


**Fig. 1.** Absorption and emission spectra of some commonly used fluorescent labels.<sup>14</sup> (a) Absorption and emission peaks of Rhodamine Red (a commonly used organic fluorescent dye) and DsRed2 (a fluorescent protein tag expressed by genetic engineering). Each dye requires a different excitation wavelength and emits fluorescence at a different wavelength. (b) Absorption and emission spectra of CdSe-core QDs indicating differences in emission peaks for CdSe-core QDs for differences in the radii of QDs for a single absorption peak. (c) Fluorescence intensities observed in actual samples.

Other important features of QDs include their long fluorescent lifetime, large molar extinction coefficient, and resistance to photobleaching.<sup>8</sup> In general, QDs fluoresce much longer (10–100 ns) compared to normal fluorophores (~2 ns) after discontinuing light excitation. This property can be used for the differentiation of QDs from other fluorophores. For example, fluorescent lifetime imaging microscopy (FLIM) can differentiate fluorescence caused by auto-fluorescence and QDs. This can be achieved by programming to start the imaging procedure a couple of nanoseconds after the discontinuation of light exposure. This delayed imaging procedure ensures that the fluorescence resulting from QDs can be detected over the auto-fluorescence. QDs have a molar absorption of  $10^5$ – $10^6$  M<sup>-1</sup> cm<sup>-1</sup> compared to that of  $2.5 \times 10^4$  to  $2.5 \times 10^5$  M<sup>-1</sup> cm<sup>-1</sup> for organic fluorescence dyes.<sup>17</sup> The higher extinction coefficients of QDs indicate that QDs are more efficient in absorbing excitation photons. Hence, they are brighter (10–20 times stronger than organic dyes), enabling the detection of lower concentrations of analytes. Furthermore, QDs are stable under exposure to a light source, which is approximately a thousand times more than organic dyes.<sup>6</sup> This unique resistance to photobleaching is particularly useful for long-term monitoring of biological processes.

### *Bioconjugation of QDs*

For biological applications, QDs need to be conjugated with biomolecules without changing the molecular structure. A number of strategies have been reported to conjugate biomolecules to QDs, including biotin–streptavidin binding,<sup>18</sup> electrostatic interaction,<sup>19</sup> mercapto exchange,<sup>20</sup> and cap exchange.<sup>21</sup> One of the simplest conjugation methods is to coat QDs with avidin.<sup>11</sup> Avidin-coated QDs can be further attached to biotin-tagged biomolecules, including antibodies and nucleic acids. Due to the high affinity between biotin and streptavidin, desired biomolecules can be reliably attached onto the surface of QDs. Currently, avidin-conjugated QDs of different fluorescent wavelengths are commercially available. Although the biotin–avidin conjugation method is simple and reliable, it also has some disadvantages. First, avidin molecules are bulky (~60 kDa), and can cause several steric effects. Second, avidin-coated QDs tend to aggregate. Third, cross-linking of the surface proteins also becomes a concern considering the fact that there are up to 40 biotin binding sites.<sup>22</sup> To overcome these disadvantages, monovalent streptavidin were conjugated with size-reduced QDs so that they bind to biotinylated biomolecules at a ratio of 1:1.<sup>22</sup>

Another way for bioconjugating QDs is electrostatic exchange. Biomolecules can be adsorbed to the hydrophilic shell through electrostatic interactions.<sup>18</sup> Mattoussi and co-workers demonstrated the conjugation of positively charged QDs to the negatively charged surfaces of the biomolecules. This method showed high stability, high yield (higher than that of non-conjugated counterparts), and little or no particle aggregation. Using the same strategy, engineered proteins can be attached to QDs for biomolecule binding. Goldman *et al.* demonstrated the conjugation of IgG antibodies to QDs via protein G.<sup>19</sup> In this method, antibodies bind to QDs through their Fc (Fragment, crystallizable) region and position their Fab sites outward, which can lead to the favorable orientation of antibodies for maximum antibody–antigen interactions.

Alternatively, biomolecules can be conjugated to the surface of QDs through a mercapto exchange process.<sup>23</sup> In this process, biomolecules containing thiol (–SH) groups can attach to the shell of QDs. The resulting bioconjugate, however, is not as stable as the other two bioconjugation methods mentioned earlier. The attached biomolecules do not have a strong bond with QDs and they can be easily detached from QDs. The mercapto exchange process also requires the use of strong organic solvents, e.g., DMSO, that negatively affect QD structures and biological components conjugated to QDs. To improve stability, dative thiol binding can be used to link the cysteine residues of the biomolecule and QDs.<sup>24</sup>

QDs can also be conjugated to biomolecules by modifying the surface QDs with functional groups.<sup>19</sup> This process, known as cap exchange, involves the usage of a cross-linker molecule to bind to the QD, while exposing the desired functional groups on the outer layer. To link QDs and the desired biomolecules, bifunctional cross-linkers with two main ligands — one attaching to the QDs (e.g., thiol group), and the other attaching to the biomolecule of interest (–COOH, –NH<sub>2</sub>, –SH) — are used. Biomolecule–QD complexes made by this process are much more stable than those made by the mercapto exchange process.<sup>11,25</sup> Two commonly used cross-linking agents are 1-ethyl-3-(3-dimethylaminopropyl)carbodiimide (EDC) and N-hydroxysuccinimide ester (NHS).<sup>26</sup> EDC can link –NH<sub>2</sub> and –COOH groups, while SMCC links –SH and –NH<sub>2</sub> groups.

Another specific cross-linker is the nickel–nitrilotriacetic acid complex (Ni–NTA), which is used for histidine-tagged peptides and antibodies.<sup>27</sup> The nitriloacetic acid group covalently binds to the carboxyl group on the QD, while the histidine-tagged antibodies bind to nickel ions.<sup>28</sup> This method is favorable over the biotin–avidin method because of low production costs. Further, histidine-expressing molecules can be directly attached to QDs with Zn<sup>2+</sup>.

## Application of QDs for Fluorescence Imaging

### *Use of QDs for cellular imaging in vitro*

Standard microscopy does not permit the direct visualization of cellular structures, as they are too small and transparent to be visualized and thus, these cells are generally labeled with a fluorescent biomarker to facilitate microscale visualization via fluorescent microscopy. It is expected that QDs will replace the conventional fluorophores for cellular imaging and multiplex tissue imaging due to their appealing optical properties. For example, QDs have successfully labeled cellular components such as nuclear proteins, mitochondria, microtubules, actin filaments, endocytic compartments, mortalin, and cytokeratin, as well as cellular membrane proteins and receptors such as serotonin transport proteins, prostate-specific membrane antigen, Her2, glycine receptors, erbB/HER, and P-glycoprotein.<sup>11</sup>

QDs have also been used to label molecular targets at the subcellular level. In one early study, Bruchez *et al.* demonstrated the labeling of cellular actin fibers with biotin-conjugated QDs.<sup>29</sup> More specifically, F-actin filaments were labeled by red QDs using avidin–biotin interactions for ligand–receptor binding. The preparation of this experiment involves the incubation of the fibroblasts in phalloidin–biotin and streptavidin, then labeling them with QDs with covalently conjugated biotin. The positive results of this experiment marked that QDs can be successfully used to label subcellular targets. However, the QDs bound non-specifically to the nuclear membrane in this study, but the generated signal was relatively weak.<sup>29</sup> Nie *et al.* reported the labeling of the protein transferrin and the incorporation of QDs by live cells.<sup>8</sup> More recently, Wu *et al.* performed a quantitative analysis into the labeling efficiency of QDs at the subcellular level.<sup>30</sup> In this study, QDs were conjugated with immunoglobulin G (IgG) and streptavidin. These QDs were used to label various cellular receptors and components at different subcellular locations; these experiments were performed with different types of specimens such as live cells, fixed cells, and tissue sections.<sup>30</sup> The results of this study produced high-quality multicolor labeling of different cellular structures, showing that QDs are effective in cellular imaging and multi-target cellular detection (Fig. 2).

The most direct way of using QDs for cancer cell detection as demonstrated in *in vitro* studies is the cellular labeling of cancer biomarkers. For example, it is known that the protein mortalin is located at several cellular sites and exhibits distinct staining patterns and different functional properties depending on whether the cell is normal or transformed.<sup>31</sup> As mortalin can be considered as a cancer cell marker, Kaul *et al.* compared the images of

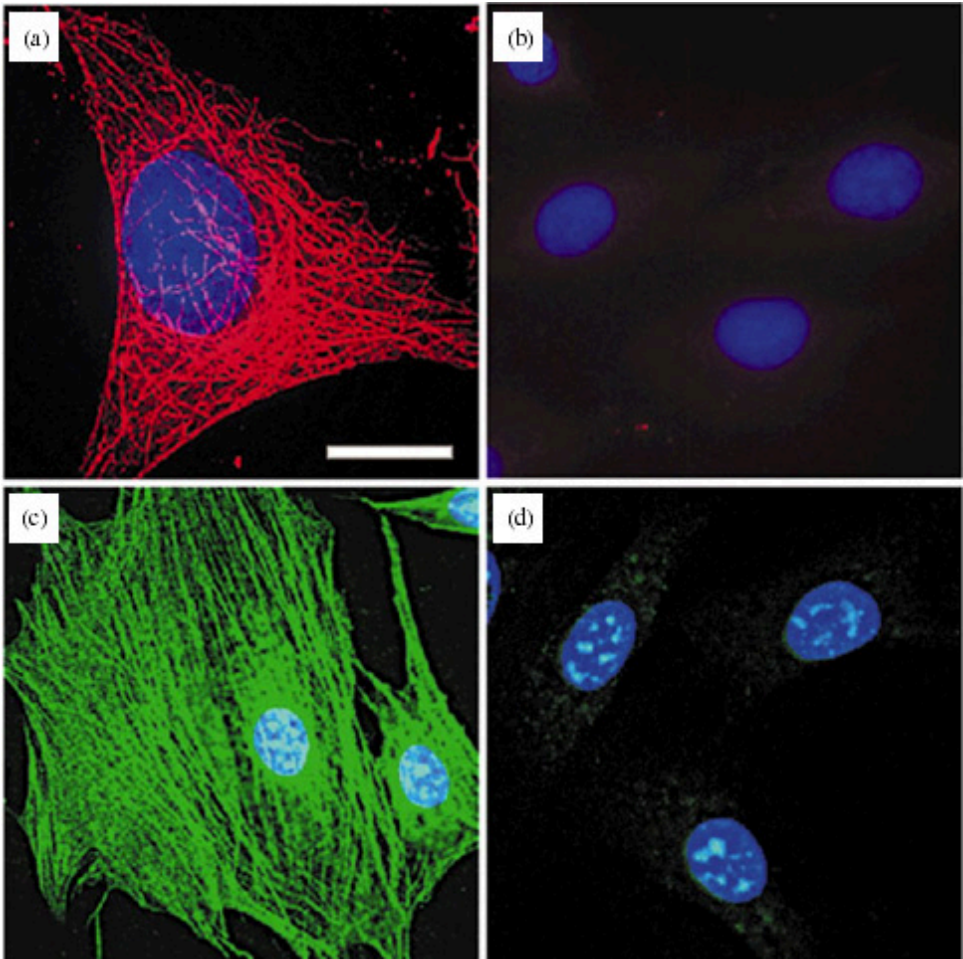


**Fig. 2.** Fluorescence staining of cytoskeleton fibers in 3T3 with streptavidin-coated QDs.<sup>31</sup> (a) Microtubules were stained with monoclonal anti- $\alpha$ -tubulin antibody, biotinylated anti-mouse IgG, and streptavidin-coated QDs (630 nm; red). (b) Control for (a): no primary antibody. (c) Actin filaments were stained with biotinylated phalloidin and streptavidin-coated QDs (535 nm; green). (d) Control for (c): no biotin-phalloidin. Cell nuclei were counterstained with Hoechst 33342 blue dye. Scale bar: 10  $\mu$ m for (a), 24  $\mu$ m for (b)–(d).

mortalin through the use of conjugated QDs.<sup>32</sup> Wu *et al.* used their aforementioned QDs conjugated with IgG and streptavidin to label HER2, a breast cancer biomarker.<sup>30</sup> The labeling of HER2 by the QD–IgG probes was successful and proved that the QD–IgG conjugates are specific toward their targets. In addition, QD–streptavidin conjugates have a low non-specific binding when there is no primary antibody in the system.<sup>30</sup>

QDs have also been used in research pertaining to the massive and rapid screening of proteins and nucleic acids. Han *et al.* encoded polymer microbeads with QDs at precise ratios to analyze biological molecules in parallel.<sup>33</sup> These results demonstrated that single-color encoded beads produced accuracies as high as 99.99%. Fluorescence staining of fixed cells with QDs allows the enhancement of fluorescence imaging because of the enlarged pore size on the cell surface and relatively free entry of QDs into the cells. For example, Lidke *et al.* stained epidermal growth factor with QDs (EGF-QDs) to image and analyze erbB/HER signal transduction.<sup>34</sup> EGF-QDs were prepared using size-exclusion (40 kDa) spin columns (Biorad). The significance of these experiments can be appreciated in light of the fact that the EGF-QDs bound to filopodial erbB1 and revealed a novel mechanism of retrograde transport to the cell body. Thus, QDs can be used as a fluorescence probe to explore protein-protein interactions.<sup>34</sup>

Further, QDs have also been used to facilitate rapid CD4<sup>+</sup> T lymphocyte counting using microfluidic devices.<sup>35,36</sup> In this method, anti-CD4 and anti-CD8 antibodies were conjugated to QDs via biotin-avidin interaction. When CD4<sup>+</sup> T lymphocytes were captured by antibodies coated on microchannel surface (for more information on this strategy, see Chapter 17), anti-CD4 and anti-CD8 antibody-conjugated QDs were used to achieve fluorescence imaging/counting (Fig. 3). This study demonstrated that the QD-based CD4<sup>+</sup> T lymphocyte counting system can be potentially used in resource-constrained settings, since CD4 cell count (flow cytometry) and viral load measurement (RT-qPCR) are expensive (US\$50–200 per test).<sup>37</sup>

### *Use of QDs for cellular imaging in vivo*

*In vivo* studies face the challenge of delivering the QDs through the cell membrane lipid bilayer without damaging cellular unity. Several methods have been developed that overcome this obstacle, including endocytic uptake, scrape loading, microinjection, electroporation, and mediated targeted uptake.<sup>14,38</sup> Through these methods, it is possible to label cells and image them for longer time intervals.<sup>38</sup> In addition, antibody-coated QDs improved biocompatibility for biological applications.<sup>35,39,40</sup> Another possibility is the encapsulation of individual QDs in phospholipid micelles.<sup>41</sup> These micelle-encapsulated QDs were successfully used in *in vivo* experiments of *Xenopus* embryos with better biocompatibility. However, the degradation of phospholipid micelles is still unknown. This method seems to be an attractive platform for targeting cells due to the small size and biocompatibility of lipids.

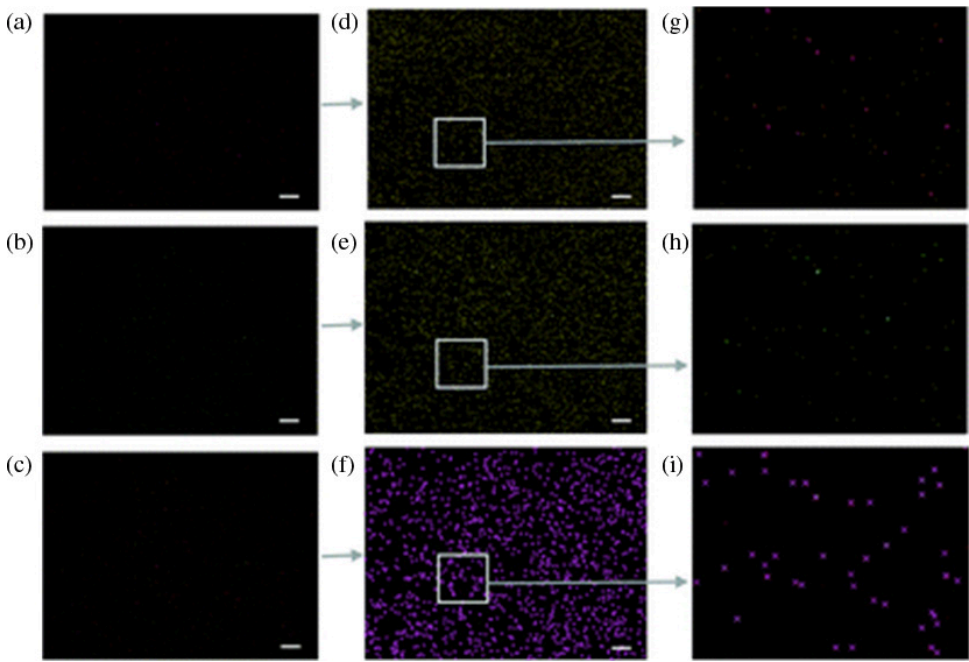


**Fig. 3.** Fluorescence imaging of CD4<sup>+</sup> T lymphocytes on a microchip.<sup>36</sup> The captured CD4<sup>+</sup> T lymphocytes were stained AF488-anti CD3 (a) and AF647-anti CD4 (b). To facilitate rapid counting, fluorescence images were merged for better recognition by a counting algorithm (c). Images (d)–(f) were processed and counted by the counting algorithm. Images (g)–(i) are the corresponding portions that were shown in images of (d)–(f), respectively.

Multicolor imaging of human prostate cancer cells grown in mice after systemic injection was reported by Gao *et al.*<sup>42</sup> The QDs used in this study contained an amphiphilic triblock copolymer, targeting ligands and multiple polyethylene glycol (PEG) molecules. The prepared QDs were capable of specific cancer cell labeling, while at the same time, possessed steady *in vivo* protection and improved biocompatibility. Due to the use of an ABC triblock polymer, QDs did not experience fluorescence loss and particle aggregation that occurred in QDs in *in vivo* experiments. This study produced images of simultaneous multicolor QDs accumulating on a tumor cell growing area. To visualize and monitor tumor cells, two different mechanisms (active and passive) were performed. The active mechanism was found to be much faster and more efficient than passive targeting. It was also noted that there was no fluorescent emission available from the tumor when hydroxylated QDs were used, indicating a rapid blood clearance by the reticuloendothelial system. The use of PEGylated QDs and QDs with prostate-specific membrane antigen-specific monoclonal antibodies both showed QD accumulation at the

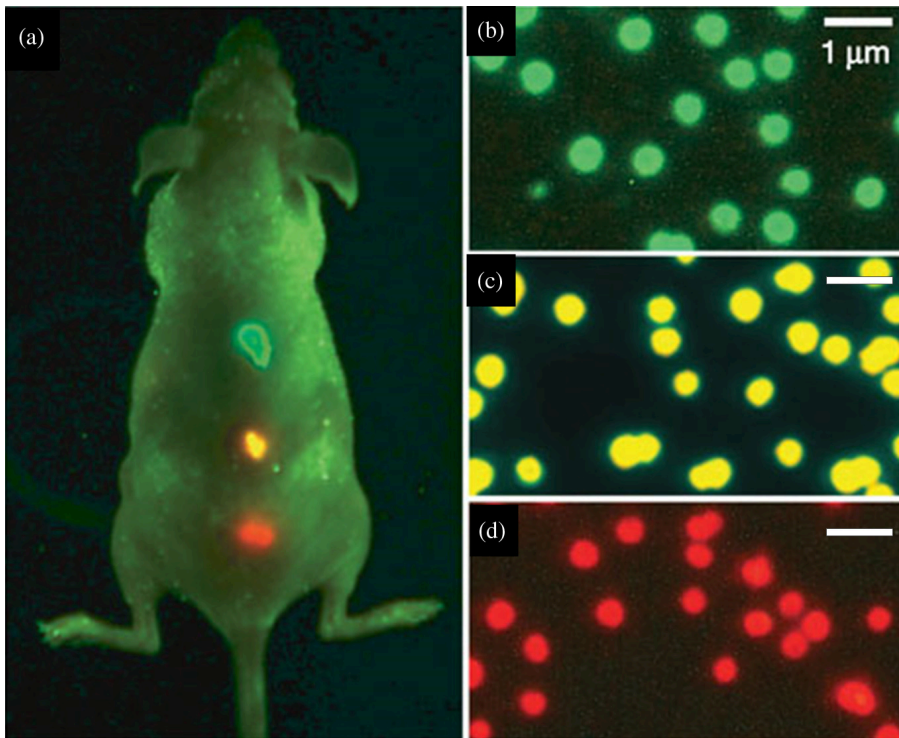


**Fig. 4.** Simultaneous *in vivo* imaging of multicolor QD-encoded microbeads.<sup>42</sup> QD-encoded microbeads (0.5  $\mu\text{m}$  diameter) were injected into a single mouse at three different locations (a). They emitted green, yellow, or red light, which was observed simultaneously with a single light source in (b)–(d), respectively.

tumor site (Fig. 4). These results demonstrated the importance of considering surface charges and/or ligands on the QDs when employing them for *in vivo* experiments.

*In vivo* studies of cancer cells in animals showed that specifically conjugated QDs accumulate at tumor sites, which can be used to image and monitor the diseased cancer tissue. Cai *et al.* reported the successful imaging of tumor vasculatures using QDs conjugated with arginine–lysine–aspartic acid peptides.<sup>43</sup> Peptides attached to QDs hold more promise as target ligands over QD–antibody conjugates due to the fact that many peptides could be attached to the QD’s surface simultaneously. This resulting polyvalency effect, defined as acting against or interacting with more than one valence, creates a stronger interaction between the QD and the target molecule.<sup>44</sup> Integrin  $\alpha_v\beta_3$  was overexpressed on activated tumor cells in this study since it binds to the RGD-containing motifs of the interstitial matrix. Other studies have previously suggested that integrin  $\alpha_v\beta_3$  can serve as a target for tumor

imaging since it causes tumor angiogenesis and thus tumor metastasis.<sup>45</sup> Stroh *et al.* combined multiphoton microscopy and QDs in their experiment to visually differentiate tumor vessels from perivascular cells and the matrix.<sup>46</sup> They also succeeded in observing the activities of the precursor cells and examining the capability of particles to access the tumor sites. Similar experiments were performed by Voura *et al.*, where QDs were used to track tumor cells in the process of metastasis.<sup>47</sup>

### *Application of QDs for viral tracking/detection*

QDs have been extensively used for virological applications and viral detection. One of the applications is to continuously track the viral infection and to understand its progression. Continuous tracking of viral infection at the early phases can provide insightful information on the mechanism of the infection and offer potential opportunities for anti-viral drug and vaccine development. Long-term tracking of single viral particles was made possible by utilizing the photostability and brightness properties of QDs.<sup>48</sup>

Agrawal *et al.* first demonstrated the possibility of covalently attaching QDs to the surface of viral particles.<sup>49</sup> Then, Joo *et al.* also demonstrated that retroviruses such as the human immunodeficiency virus (HIV) can be successfully tagged with QDs through the membrane incorporation of a short acceptor peptide, which is susceptible to site-specific biotinylation and attachment of streptavidin-conjugated QDs.<sup>50</sup> In this approach, a biotinylated 15-amino acid peptide was first incorporated onto the surface of a virion.<sup>50,51</sup> This application enabled QD labeling for visualizing the dynamic interactions between viruses and target cells so as to study how different types of retroviruses enter the host cell, which helps in the understanding of viral infections. However, this method requires the careful positioning of the QDs onto the viral capsid proteins to avoid non-specific binding of QDs.<sup>49</sup> Dixit *et al.* demonstrated the incorporation of CdSe/ZnS semiconductor QDs into viral particles.<sup>52</sup> The encapsulation of functionalized QDs was achieved by the self-assembly of HS-PEG-COOH-tagged DNA sequence in viral capsids, which yielded a virus-like particle similar in size to native viral particles.<sup>52</sup>

In addition, QDs have been used to achieve the rapid detection of HIV on a chip.<sup>40</sup> It requires only a finger-prick volume (10  $\mu$ L) of unprocessed HIV-infected whole blood and a microfluidic chip immobilizing an antibody against the viral envelope protein gp120. The use of two different-colored QDs allows the application of a dual-stain imaging technique and provides a new and effective tool for the accurate detection of HIV particles (Fig. 5).

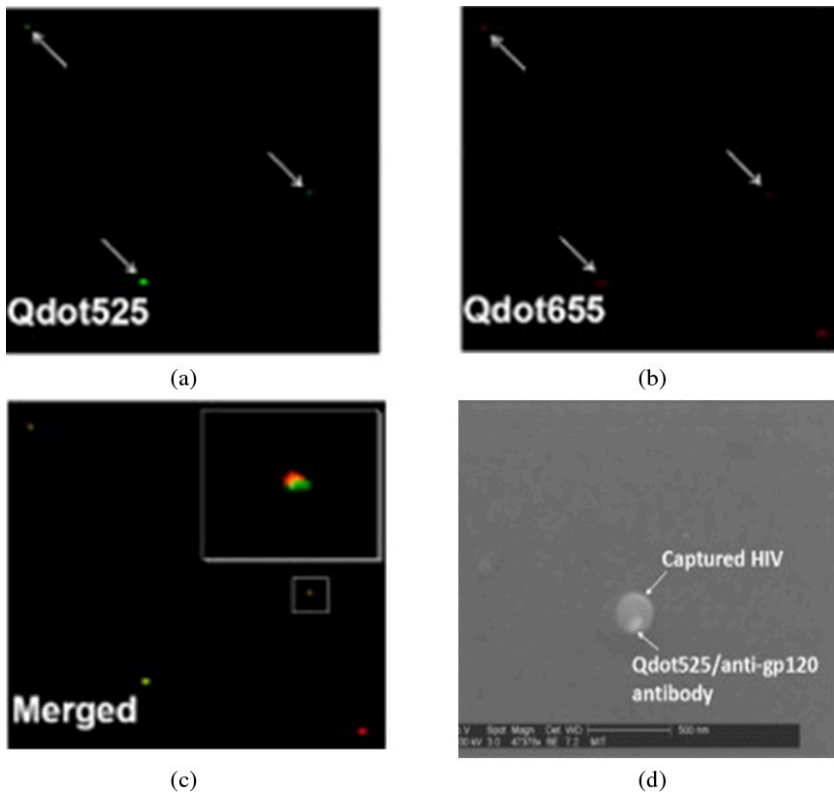


**Fig. 5.** Fluorescence imaging of HIV particles using QDs.<sup>40</sup> HIV particles were captured by anti-gp120 antibodies, which were coated on the microchannel surface. For dual-staining, streptavidin coated QDs (green QDs 525 and red QDs 655) were used to identify biotinylated ConA and anti-gp120 antibody via streptavidin–biotin interaction. These two QDs were sequentially introduced into the channel to achieve the specific detection of gp120 (a) and high-mannose oligosaccharide (b) on the viral surface. Using these two specific and independent reactions between gp120 and anti-gp120, and between mannose and ConA lectin, HIV-1 particles were specifically detected by co-recognition (c). The captured HIV particle was also confirmed via scanning electron microscopy (d).

This microfluidic device can be potentially used for HIV detection and viral load monitoring in resource-limited settings.<sup>40</sup>

QDs have also been successfully used for the detection of hepatitis B virus (HBV) DNA in a nanobiosensor that is simple, specific, rapid, and with high throughput.<sup>53</sup> This QD–DNA nanosensor is based on fluorescence resonance energy transfer (FRET). It is capable of detecting the target DNA and even a single mismatch in the HBV genome. In this application, water-soluble CdSe/ZnS QDs were first prepared by replacing the trioctylphosphine oxide on the surface with 3-mercaptoproionic acid. Then, functional QD–DNA

conjugates were formed by the attachment of oligonucleotides onto the surface. To form QD–DNA-conjugated sandwich hybrids, DNA targets and Cy5-modified signal DNAs were added. The fluorescence emission resulting from Cy5 fluorophore (the acceptor) and QD (the donor) was captured by a FRET microscope. No Cy5 emission was produced due to the lack of FRET in the case of a single-base mismatch. Wang *et al.* showed that this method can be used for the high-throughput and multiplexed detection of target HBV DNA and its mutations.<sup>53</sup>

Another experiment on viral detection done by Liang *et al.* combined two-photon microscopy with hepatitis C virus (HCV)-specific QDs that were conjugated as fluorescent tags.<sup>54</sup> The study demonstrated the feasibility of detecting HCV-infected cells using QDs, and their extent and distribution within the liver of patients who have chronic HCV infection. QDs specific to HCV infected cells were used to determine the proportion of HCV-infected hepatocytes and healthy ones. Liang *et al.* showed that the QD application is able to detect the viral core and non-structural protein 3 antigens from patient liver tissues that are infected with HCV.

## **Toxicity and Biosafety of QDs**

Although QDs have been widely used for applications in biological imaging, studies on their potential toxicity to human beings, animals, plants, as well as the environment have not been extensively carried out.<sup>55</sup> Recently, concerns about the potential hazards that QDs pose toward both humans and the environment are gradually gaining attention.<sup>56,57</sup> It is essential to understand environmental concerns and the cytotoxicity of using QDs before applying them in the clinical arena. In the following section, the potential toxicity and biosafety considerations of QDs will be discussed.

### ***Potential toxicity of QDs***

The toxicity of QDs depends on various factors derived from their inherent physicochemical properties and environmental conditions. Properties such as size, concentration, surface coating (capping material and functional groups), dispersibility, species, and exposure time are associated with QD toxicity.<sup>58</sup> As a result, both the intrinsic properties of QDs and the surrounding environmental conditions should be considered to evaluate QD toxicity.

Two important parameters, i.e., QD size and dose, have been associated with QD cytotoxicity. The QD size (typically ranging from 5 to 50 nm) is critical to the biological response of cells. Smaller QDs (< 2.5 nm) tend to

localize in and around the cell nucleus, whereas larger QDs are typically distributed within the cytoplasm.<sup>59,60</sup> Lovric *et al.* showed that the size of QDs is related to their subcellular distribution and the severity of QD-induced cytotoxicity.<sup>60</sup> In addition, the dose is also an important factor due to the large influence of surface area to QD actions. A significant decrease in cell viability was observed even at a low concentration (0.1 mg/mL) of QDs, and smaller-sized QDs have been shown to have stronger effects on the death rate of exposed cells due to accumulation around the nucleus and their higher mobility inside the cell.<sup>61</sup> It has also been reported that the cell death rate is time-dependent,<sup>59</sup> indicating that long-term cytotoxicity needs to be studied.

The surface modification of QDs also plays a predominant role in determining QD toxicity. Some compounds such as mercaptoundecanoic acid (MUA) coated on QDs are responsible for genotoxicity.<sup>62</sup> Other surface modifications on QDs, such as the capping material, can also affect the internalization of QDs into the cells. For instance, smaller green fluorescent QDs (~13 nm) were observed inside breast cancer cells when using MPA-polymer- and polymer-silane-coated QDs. In contrast, larger red fluorescent QDs (~24 nm) were barely detected inside the cells. However, the exact opposite results were observed for PEG-silane-coated QDs. Hence, the toxicity of QDs to different cells depends on the size of the QD.<sup>39</sup> Although the detailed mechanisms remain to be explored, studies have shown that the toxic effects may result from the precipitation of Cd<sup>2+</sup> ions on the cell surface, where the release of toxic molecules from the surface modification of QDs resulted in cellular and/or nuclear lipid membrane damage.<sup>62,63</sup>

The environmental conditions containing QD suspensions can also directly affect cell viability. For instance, a study indicated that cell viability dramatically decreases, if the QDs are initially exposed to air for 30 min,<sup>64</sup> which may be due to the oxidation of the QD surface, releasing a high level of free Cd<sup>2+</sup> ions. As reported, Cd<sup>2+</sup> ions cause severe kidney disorders by affecting the Na<sup>+</sup>/glucose co-transporter on the renal cell membrane.<sup>65</sup> Similar toxicity results were obtained with an increase in UV radiation exposure time.<sup>66</sup> Evidence has shown that the release of these free radical ions is detrimental to cells. Some antioxidants were found to be able to inhibit cytotoxicity by controlling the shell structure of QDs and preventing the QDs from degradation.<sup>60</sup> Further studies are required to fully understand the influence of the environment on QDs. In addition, studies have shown that current two-dimensional cultures are not efficient in indicating the cytotoxicity of QDs *in vivo*. When a three-dimensional cell culture model of liver tissue was used, the QD's toxic effects are significantly reduced as compared to two-dimensional cultures.<sup>67</sup> The significant reduction of cytotoxicity in

three-dimensional cultures compared to two-dimensional cultures is due to the well-developed layer of the extracellular matrix (ECM), which decreases the amount of QDs from entering inner layers of cells. In two-dimensional cultures, there is no ECM acting as a protective barrier.<sup>67</sup>

Several *in vivo* studies performed on rats illustrated different absorbance and clearance rates of QDs after intravenous injection, which differed in types, sizes, and surface modifications.<sup>68-70</sup> However, a common finding is that the liver is the organ where xenobiotics, e.g., QDs, accumulate the most. Interestingly, no significant changes of physiological or pathological parameters were observed in the target tissues.<sup>59</sup> Nevertheless, the current number of studies performed *in vivo* is not sufficient to draw conclusions of QD toxicity *in vivo*. Investigations should be made on QD distribution, excretion, metabolism, pharmacokinetics, and pharmacodynamics in animal models *in vivo*, which will be vital for the development of QD-based clinical applications, such as *in vivo* fluorescence imaging and monitoring drug delivery.

### *Biosafety of QDs*

The potential routes of QD exposure to human include environmental, workplace, and therapeutic or diagnostic administration during their development, manufacture, usage, and disposal.<sup>58,71</sup> Most common routes of QD exposure include inhalation, dermal contact, or ingestion. Inhalation is thought to be one of the most important routes of all nanoparticle exposure, including QDs, since nanoparticles can travel great distances in air through Brownian motion.<sup>71</sup> The QDs' size plays a significant role in terms of their deposition in pulmonary tissues upon inhalation. For example, QDs smaller than 2.5 nm could potentially reach deeper into lungs and interact with the alveolar epithelium, whereas larger aerosolized QDs would deposit in bronchial spaces. However, little is known about the aerosolization of QDs in air, in which QDs of smaller size may form aggregates, thus increasing their size.

The interaction of QDs with the skin was also studied. One study demonstrated that QDs can barely penetrate the skin layer. In this study, a small fraction of several QDs species was shown to pass through the stratum corneum, with an even smaller fraction accumulating within the dermis. The penetration is dependent on the size, shape, and surface charge of the QDs, with smaller and spherical QDs appearing to penetrate deeper. None of the QDs were found to be able to penetrate through the entire thickness of the skin, indicating that healthy, intact skin should act as a sufficient barrier to some QDs.<sup>72</sup> However, further studies are needed to better understand the penetration of QDs into intact and diseased skin.

The ingestion of QDs is also possible through inhaling QDs or hand-to-mouth transfer of QDs. Like other nanoparticles, QDs may undergo limited ingestion absorption, mainly to the lymphoid system following systemic exposure. Data suggest that the absorption of QDs through ingestion is governed by the size and the surface characteristics of the particle (with increased absorption for smaller, hydrophobic, and neutral particles).<sup>73,74</sup>

## Summary and Perspectives

QDs, owing to their superior optical properties to conventional organic dyes, have been widely used as fluorescent tags to facilitate biomedical imaging *in vitro* and *in vivo*. For a wide range of applications, a variety of bioconjugation methods such as biotin–avidin-based electrostatic interaction, as well as thiol chemistry-based mercapto exchange and cap exchange are available. These bioconjugation technologies enable versatile applications of QDs in fluorescence labeling and imaging. Through QD-based fluorescence technologies, the visualization of subcellular components, whole cells, transport processes, tumor propagation, and viruses has been achieved. Multiplex imaging of cellular components (such as nuclear proteins, mitochondria, microtubules, endocytic compartments, and serotonin transport proteins) is a distinct advantage offered by QDs. Thus, QDs hold great potential to be further utilized to probe unknown proteins or nucleic acids in basic research.

QD-based medical imaging has also been used to facilitate the diagnosis of cancer and infectious diseases. One of the future research goals is to develop QD-based biosensors to deliver point-of-care diagnostics. This aspect is particularly important to achieve the diagnosis and monitoring of infectious diseases in resource-constrained settings. The other future research direction will be investigating the cytotoxicity of QDs both *in vitro* and *in vivo*. Clinical application of QDs cannot be achieved until the pros and cons in medical imaging *in vivo* are well characterized. In addition, emphasis should be placed on the evaluation of QD toxicity to human beings, animals, plants, as well as the ecosystem. Furthermore, environmental effects on QD toxicity should be considered in the aspects of chemical modifications, electrostatic interactions, and cellular targets.

## References

1. Morgan, T.T. *et al.*, Encapsulation of organic molecules in calcium phosphate nanocomposite particles for intracellular imaging and drug delivery. *Nano Lett.*, 2008. **8**(12): p. 4108–4115.

2. Tosi, S. *et al.*, Classification of deletions and identification of cryptic translocations involving 7q by fluorescence *in situ* hybridization (FISH). *Leukemia*, 1996. **10**(4): p. 644–649.
3. Jain, R.K., Stroh, M., Zooming in and out with quantum dots. *Nat Biotechnol*, 2004. **22**(8): p. 959–960.
4. Bruchez, M. *et al.*, Semiconductor nanocrystals as fluorescent biological labels. *Science*, 1998. **281**(5385): p. 2013–2016.
5. Chan, W.C.W. *et al.*, Luminescent quantum dots for multiplexed biological detection and imaging. *Curr Opin Biotechnol*, 2002. **13**(1): p. 40–46.
6. Xing, Y. *et al.*, Bioconjugated quantum dots for multiplexed and quantitative immunohistochemistry. *Nat Protoc*, 2007. **2**(5): p. 1152–1165.
7. Bruchez, M., Jr. *et al.*, Semiconductor nanocrystals as fluorescent biological labels. *Science* 1998. **281**(5385): p. 2013–2016.
8. Chan, W.C., Nie, S., Quantum dot bioconjugates for ultrasensitive nonisotopic detection. *Science*, 1998. **281**(5385): p. 2016–2018.
9. Murray, C.B., Kagan, C.R., Bawendi, M.G., Synthesis and characterization of monodisperse nanocrystals and close-packed nanocrystal assemblies. *Annu Rev Mater Sci*, 2000. **30**: p. 545–610.
10. Hines, M.A., Guyot-Sionnest, P., Synthesis and characterization of strongly luminescing ZnS-Capped CdSe nanocrystals. *J Phys Chem*, 1996. **100**(2): p. 468–471.
11. Medintz, I.L. *et al.*, Quantum dot bioconjugates for imaging, labelling and sensing. *Nat Mater*, 2005. **4**(6): p. 435–446.
12. Klimov, V.I., Optical gain and stimulated emission in nanocrystal quantum dots. *Science*, 2000. **290**(5490): p. 314–317.
13. Alivisatos, A.P., Semiconductor clusters, nanocrystals, and quantum dots. *Science*, 1996. **271**(5251): p. 933–937.
14. Medintz, I.L. *et al.*, Quantum dot bioconjugates for imaging, labelling and sensing. *Nat Mater*, 2005. **4**(6): p. 435–446.
15. Yoffe, A.D., Semiconductor quantum dots and related systems: Electronic, optical, luminescence and related properties of low dimensional systems. *Adv Phys*, 2001. **50**(1): p. 1–208.
16. Jaiswal, J.K. *et al.*, Long-term multiple color imaging of live cells using quantum dot bioconjugates. *Nat Biotechnol*, 2003. **21**(1): p. 47–51.
17. Resch-Genger, U. *et al.*, Quantum dots versus organic dyes as fluorescent labels. *Nat Methods*, 2008. **5**(9): p. 763–75.
18. Goldman, E.R. *et al.*, Avidin: A natural bridge for quantum dot-antibody conjugates. *J Am Chem Soc*, 2002. **124**(22): p. 6378–6382.
19. Mattoussi, H. *et al.*, Self-assembly of CdSe–ZnS quantum dot bioconjugates using an engineered recombinant protein. *J Am Chem Soc*, 2000. **122**(49): p. 12142–12150.
20. Willard, D.M. *et al.*, CdSe–ZnS quantum dots as resonance energy transfer donors in a model protein–protein binding assay. *Nano Lett*, 2001. **1**(9): p. 469–474.
21. Mitchell, G.P., Mirkin, C.A., Letsinger, R.L., Programmed assembly of DNA functionalized quantum dots. *J Am Chem Soc*, 1999. **121**(35): p. 8122–8123.
22. Howarth, M. *et al.*, Monovalent, reduced-size quantum dots for imaging receptors on living cells. *Nat Methods*, 2008. **5**(5): p. 397–399.
23. Parak, W.J. *et al.*, Biological applications of colloidal nanocrystals. *Nanotechnology*, 2003. **14**(7): p. R15–R27.

24. Pinaud, F. *et al.*, Bioactivation and cell targeting of semiconductor CdSe/ZnS nanocrystals with phytochelatin-related peptides. *J Am Chem Soc*, 2004. **126**(19): p. 6115–6123.
25. Uyeda, H.T. *et al.*, Synthesis of compact multidentate ligands to prepare stable hydrophilic quantum dot fluorophores. *J Am Chem Soc*, 2005. **127**(11): p. 3870–3878.
26. Alivisatos, A.P., Gu, W., Larabell, C., Quantum dots as cellular probes. *Annu Rev Biomed Eng*, 2005. **7**: p. 55–76.
27. Hainfeld, J.F. *et al.*, Ni-NTA-gold clusters target His-tagged proteins. *J Struct Biol*, 1999. **127**(2): p. 185–198.
28. Xu, C. *et al.*, Nitrotriacetic acid-modified magnetic nanoparticles as a general agent to bind histidine-tagged proteins. *J Am Chem Soc*, 2004. **126**(11): p. 3392–3393.
29. Bruchez, M., Jr. *et al.*, Semiconductor nanocrystals as fluorescent biological labels. *Science*, 1998. **281**: p. 2013–2016.
30. Wu, X. *et al.*, Immunofluorescent labeling of cancer marker Her2 and other cellular targets with semiconductor quantum dots. *Nat Biotechnol*, 2003. **21**(1): p. 41–46.
31. Wadhwa, R. *et al.*, Differential subcellular distribution of mortalin in mortal and immortal mouse and human fibroblasts. *Exp Cell Res*, 1993. **207**(2): p. 442–448.
32. Kaul, Z. *et al.*, Mortalin imaging in normal and cancer cells with quantum dot immun-conjugates. *Cell Res*, 2003. **13**(6): p. 503–507.
33. Han, M. *et al.*, Quantum-dot-tagged microbeads for multiplexed optical coding of biomolecules. *Nat Biotechnol*, 2001. **19**(7): p. 631–635.
34. Lidke, D.S. *et al.*, Quantum dot ligands provide new insights into erbB/HER receptor-mediated signal transduction. *Nat Biotechnol*, 2004. **22**(2): p. 198–203.
35. Jokerst, J.V. *et al.*, Integration of semiconductor quantum dots into nano-bio-chip systems for enumeration of CD4+T cell counts at the point-of-need. *Lab Chip*, 2008. **8**(12): p. 2079–2090.
36. Alyassin, M.A. *et al.*, Rapid automated cell quantification on HIV microfluidic devices. *Lab Chip*, 2009. **9**(23): p. 3364–3369.
37. Wang, S., Xu, F., Demirci, U., Advances in developing HIV-1 viral load assays for resource-limited settings. *Biotechnol Adv*, 2010. **28**(6): p. 770–781.
38. Jaiswal, J.K. *et al.*, Long-term multiple color imaging of live cells using quantum dot bioconjugates. *Nat Biotechnol*, 2003. **21**(1): p. 47–51.
39. Sukhanova, A. *et al.*, Biocompatible fluorescent nanocrystals for immunolabeling of membrane proteins and cells. *Anal Biochem*, 2004. **324**(1): p. 60–67.
40. Kim, Y.G. *et al.*, Quantum dot-based HIV capture and imaging in a microfluidic channel. *Biosens Bioelectron*, 2009. **25**(1): p. 253–258.
41. Dubertret, B. *et al.*, *In vivo* imaging of quantum dots encapsulated in phospholipid micelles. *Science*, 2002. **298**(5599): p. 1759–1762.
42. Gao, X. *et al.*, *In vivo* cancer targeting and imaging with semiconductor quantum dots. *Nat Biotechnol*, 2004. **22**(8): p. 969–976.
43. Cai, W. *et al.*, Peptide-labeled near-infrared quantum dots for imaging tumor vasculature in living subjects. *Nano Lett*, 2006. **6**(4): p. 669–76.
44. Mammen, M., Choi, S.K., Whitesides, G.M., Polyvalent interactions in biological systems: Implications for design and use of multivalent ligands and inhibitors. *Angew Chem Int Edn*, 1998. **37**(20): p. 2755–2794.
45. Liu, Z., Wang, F., Chen, X., Integrin alpha(v)beta(3)-targeted cancer therapy. *Drug Dev Res*, 2008. **69**(6): p. 329–339.

46. Stroh, M. *et al.*, Quantum dots spectrally distinguish multiple species within the tumor milieu *in vivo*. *Nat Med*, 2005. **11**(6): p. 678–682.
47. Voura, E.B. *et al.*, Tracking metastatic tumor cell extravasation with quantum dot nanocrystals and fluorescence emission-scanning microscopy. *Nat Med*, 2004. **10**(9): p. 993–998.
48. Michalet, X. *et al.*, Quantum dots for live cells, *in vivo* imaging, and diagnostics. *Science*, 2005. **307**(5709): p. 538–544.
49. Agrawal, A., Sathe, T., Nie, S., Single-bead immunoassays using magnetic micro-particles and spectral-shifting quantum dots. *J Agric Food Chem*, 2007. **55**(10): p. 3778–3782.
50. Joo, K.I. *et al.*, Site-specific labeling of enveloped viruses with quantum dots for single virus tracking. *ACS Nano*, 2008. **2**(8): p. 1553–1562.
51. Beckett, D., Kovaleva, E., Schatz, P.J., A minimal peptide substrate in biotin holoenzyme synthetase-catalyzed biotinylation. *Protein Sci*, 1999. **8**(4): p. 921–929.
52. Dixit, S.K. *et al.*, Quantum dot encapsulation in viral capsids. *Nano Lett*, 2006. **6**(9): p. 1993–1999.
53. Wang, X. *et al.*, QDs-DNA nanosensor for the detection of hepatitis B virus DNA and the single-base mutants. *Biosens Bioelectron*, 2010. **25**(8): p. 1934–1940.
54. Liang, Y. *et al.*, Visualizing hepatitis C virus infections in human liver by two-photon microscopy. *Gastroenterology*, 2009. **137**(4): p. 1448–1458.
55. Lewinski, N., Colvin, V., Drezek, R., Cytotoxicity of nanoparticles. *Small*, 2008. **4**(1): p. 26–49.
56. Oberdorster, G., Oberdorster, E., Oberdorster, J., Nanotoxicology: An emerging discipline evolving from studies of ultrafine particles. *Environ Health Perspect*, 2005. **113**(7): p. 823–839.
57. Nel, A. *et al.*, Toxic potential of materials at the nanolevel. *Science*, 2006. **311**(5761): p. 622–627.
58. Hardman, R., A toxicologic review of quantum dots: Toxicity depends on physicochemical and environmental factors. *Environ Health Perspect*, 2006. **114**(2): p. 165–172.
59. Zhang, Y. *et al.*, *In vitro* and *in vivo* toxicity of CdTe nanoparticles. *J Nanosci Nanotechnol*, 2007. **7**(2): p. 497–503.
60. Lovric, J. *et al.*, Differences in subcellular distribution and toxicity of green and red emitting CdTe quantum dots. *J Mol Med*, 2005. **83**(5): p. 377–385.
61. Shiohara, A. *et al.*, On the cyto-toxicity caused by quantum dots. *Microbiol Immunol*, 2004. **48**(9): p. 669–675.
62. Hoshino, A. *et al.*, Physicochemical properties and cellular toxicity of nanocrystal quantum dots depend on their surface modification. *Nano Lett*, 2004. **4** (11): p. 2163–2169.
63. Kirchner, C. *et al.*, Cytotoxicity of colloidal CdSe and CdSe/ZnS nanoparticles. *Nano Lett*, 2005. **5**(2): p. 331–8.
64. Derfus, A.M., Chan, W.C.W., Bhatia, S.N., Probing the cytotoxicity of semiconductor quantum dots. *Nano Lett*, 2004. **4**(1): p. 11–18.
65. Xia, X. *et al.*, The endogenous CXXC motif governs the cadmium sensitivity of the renal Na<sup>+</sup>/glucose co-transporter. *J Am Soc Nephrol*, 2005. **16**(5): p. 1257–65.
66. Li, J. *et al.*, The photodynamic effect of different size ZnO nanoparticles on cancer cell proliferation *in vitro*. *Nanoscale Res Lett*, 2010. **5**(6): p. 1063–71.
67. Lee, J. *et al.*, *In vitro* toxicity testing of nanoparticles in 3D cell culture. *Small*, 2009. **5**(10): p. 1213–21.

68. Ballou, B. *et al.*, Noninvasive imaging of quantum dots in mice. *Bioconjug Chem*, 2004. **15**(1): p. 79–86.
69. Fischer, H.C. *et al.*, Pharmacokinetics of nanoscale quantum dots: *In vivo* distribution, sequestration, clearance in the rat. *Adv Funct Mater*, 2006. **16**(10): p. 1299–1305.
70. Yang, R.S. *et al.*, Persistent tissue kinetics and redistribution of nanoparticles, quantum dot 705, in mice: ICP-MS quantitative assessment. *Environ Health Perspect*, 2007. **115**(9): p. 1339–43.
71. Stern, S.T., McNeil, S.E., Nanotechnology safety concerns revisited. *Toxicol Sci*, 2008. **101**(1): p. 4–21.
72. Ryman-Rasmussen, J.P., Riviere, J.E., Monteiro-Riviere, N.A., Penetration of intact skin by quantum dots with diverse physicochemical properties. *Toxicol Sci*, 2006, **91**(1): p. 159–165.
73. Hillyer, J.F., Albrecht, R.M., Gastrointestinal persorption and tissue distribution of differently sized colloidal gold nanoparticles. *J Pharm Sci*, 2001. **90**(12): p. 1927–36.
74. Jani, P. *et al.*, The uptake and translocation of latex nanospheres and microspheres after oral administration to rats. *J Pharm Pharmacol*, 1989. **41**(12): p. 809–12.